ISSN: 1813-4890

Grayscale Image Generation and Quality Assessment Based on LoRA Models: From Theory to Application in Ceramic Carving

Xiaoyan Wang [a], Yanping Tang [b], Shihan Jiang [c], Tao Liu [d, *]

School of Information Engineering, Jingdezhen Ceramic University, Jingdezhen 333403, China

[a]1944393272@qq.com, [b]1940977616@qq.com, [c]2821110319@qq.com, [d]10922475@qq.com

*Corresponding author

Abstract

This paper proposes a grayscale image generation and quality assessment method based on the LoRA model, with application validation in ceramic surface engraving modeling. First, a training pipeline for the LoRA model is designed for the grayscale image generation task, encompassing data preprocessing, model training, and optimization strategies. Then, the trained LoRA model is employed for grayscale image generation testing, followed by a preliminary quality analysis of the generated outputs. Subsequently, four image quality evaluation metrics are utilized to comprehensively assess the generation quality. Based on these evaluation results, the K-means clustering algorithm is applied to classify and predict image quality, and the performance of different algorithms is compared. Finally, the grayscale image generation and evaluation method is integrated into ceramic surface engraving modeling to validate the accuracy and practicality of the prediction results. Experimental results demonstrate that the proposed approach is highly effective in grayscale image generation and quality assessment, providing a novel solution for image processing in carving applications.

Keywords

LoRA Model, Grayscale Image Generation, Image Quality Assessment, K-Means Clustering, Ceramic Surface Engraving.

1. Introduction

Ceramic carving, as a traditional craft that embodies both cultural heritage and artistic expression, holds a significant position in China's arts and crafts and ceramic design fields. With the rising demand for personalized design and intelligent manufacturing, the digital transformation of ceramic carving has become a key driver for industrial upgrading. However, traditional manual carving relies heavily on the expertise of skilled artisans, resulting in low efficiency and limited capacity for pattern diversity and fine detail precision. These limitations make it difficult to meet the dual demands of modern industry for high efficiency, consistency, and customized design. Against this backdrop, grayscale image generation methods based on generative artificial intelligence (AIGC) offer new approaches and tools for the automatic design and rapid modeling of ceramic carving patterns. Such research carries both theoretical significance and practical application value.

In recent years, with the rapid development of deep learning and generative modeling techniques, large-scale generative models have achieved remarkable success in image synthesis, style transfer, and image editing. Diffusion models have gained widespread application in artistic creation and industrial design due to their superior performance in generating high-quality images [1]. Since the introduction of Generative Adversarial Networks (GANs) by Goodfellow et al. [2], various variants such as StyleGAN and CycleGAN have emerged, significantly improving control over image structure and style fidelity. Furthermore, multimodal Transformer architectures (e.g., DALL·E, Imagen) have demonstrated strong potential in cross-modal image generation tasks [3].

Despite these advances, mainstream generative models often suffer from high training costs, large parameter scales, and limited adaptability in domain-specific or small-sample scenarios. To address these challenges, several parameter-efficient fine-tuning techniques have been proposed. Among them, Low-Rank Adaptation (LoRA) [4]introduces low-rank updates to the weight matrices of pre-trained models while keeping most parameters frozen, thus enabling efficient transfer and customized training. LoRA has not only achieved success in natural language processing but has also shown promising performance in image generation tasks. Building upon this, our study adopts the LoRA technique to fine-tune a base image generation model for grayscale image generation tailored to ceramic carving. The goal is to achieve automated and high-precision generation of complex patterns.

Regarding image quality assessment, traditional metrics such as Peak Signal-to-Noise Ratio (PSNR) and Structural Similarity Index (SSIM) are typically full-reference methods. In contrast, Natural Image Quality Evaluator (NIQE) and BRISQUE provide no-reference evaluations and offer useful insights into image clarity and structural similarity [5]. However, in industrial applications such as ceramic carving, the functionality and suitability of the image for engraving are often not fully captured by these conventional metrics. Therefore, this study introduces a set of multidimensional indicators—namely, information entropy [6], Discrete Cosine Transform (DCT) [7], grayscale variance [8], and Tenengrad gradient [9]—to objectively assess image quality from the perspectives of texture complexity, frequency-domain characteristics, and edge sharpness [10]. Additionally, to enable automated quality classification and prediction, we employ the K-means clustering algorithm to categorize grayscale images based on quality attributes [11], thereby constructing an interpretable and intelligent evaluation framework.

Finally, based on the above image quality assessment system, this paper applies the generated grayscale images to ceramic surface engraving modeling, and verifies the correspondence between the image quality and the actual engraving effect through simulated engraving experiments. The experimental results show that the proposed LoRA-based fine-tuning generation scheme can not only generate grayscale images with high feasibility of engraving, but also has strong robustness and generalization ability in practical applications, which provides feasible paths and technical references for promoting the landing of AIGC technology in ceramic industrial design.

2. Training and Application of LoRA Model for Grayscale Images

2.1. Fundamental Principles of the LoRA Model

Low-Rank Adaptation (LoRA)[4] is an efficient approximation technique that performs low-rank decomposition on feature matrices to substantially reduce the number of trainable parameters while preserving model performance. By representing a high-dimensional feature matrix as the product of two lower-rank matrices, LoRA effectively lowers both computational and storage overhead. As a lightweight adaptation method, LoRA is commonly integrated with Stable Diffusion models, where only a small portion of parameters within the LoRA modules are updated during fine-tuning, rather than retraining the entire model. This approach not only reduces training costs but also improves adaptability and generalization in specific downstream tasks, making it highly practical for customized image generation applications.

2.2. Preparation and Preprocessing of Grayscale Image Dataset

2.2.1. Data Collection

During the construction of the grayscale image dataset, we adopted a multi-source data acquisition strategy. At the same time, we strictly complied with copyright regulations to

ISSN: 1813-4890

ensure that all patterns used were either legally authorized or confirmed to be in the public domain, thereby avoiding any infringement of intellectual property rights. In addition, we emphasized the diversity of samples to enhance the dataset's comprehensiveness and representativeness.

2.2.2. Data Preprocessing

In the data preprocessing stage, we performed a series of image processing operations on the collected grayscale images, including cropping, denoising, and format conversion, to ensure consistency in image quality. Furthermore, in order to facilitate subsequent model training, we standardized key parameters such as image dimensions and resolution. These preprocessing steps are essential for improving the usability of the dataset and the efficiency of model training.

2.3. Model Training Process and Parameter Settings

2.3.1. Training Environment

The hardware configuration used for model training includes an NVIDIA GeForce RTX 4090 Laptop GPU with 24 GB of video memory.

2.3.2. Training Procedure and Key Parameter Settings

After preparing the dataset, each training image is named in the format: number_name, where the number indicates the number of training steps for that image. In this training setup, the number is set to 10, resulting in a total of 10 × 300 = 3000 steps.

The base model used is a photorealistic model based on Stable Diffusion 1.5: dreamshaper_8.

The training dataset path is adjusted to point to the specific dataset used in this training task.

The training image resolution is set to match that of the dataset images and must be a multiple of 64.

The train_batch_size (batch size) is set to 2.

The max_train_epochs (maximum number of training epochs) is set to 20. Thus, the total number of training steps becomes 20 × 3,000 = 60,000 steps.

The learning rate is set to 0.0001.

2.4. Grayscale image generation test based on trained Lora model

In this study, Comfy UI was utilized for image generation testing. The positive prompt was set as: (relief:1.3), (gypsum sculpture), (monochrome:1.1), (grayscale:1.1), (high contrast:1.1), (sharp edges:1.1), (rim light:1.1), official art, black simple background, masterpiece, best quality, best details; the negative prompt was defined as: (((NSFW))), (((colorful))), (((color))), blurry, lowers, worst quality, shadow, realistic, reality, text, username, depth of field, (((black backgroom))).The prompt relevance score was set to 8. The output image resolution was 1024×1024, with 35 inference steps. The effect of grayscale image generation is shown in **错误!未找到引用源。**.

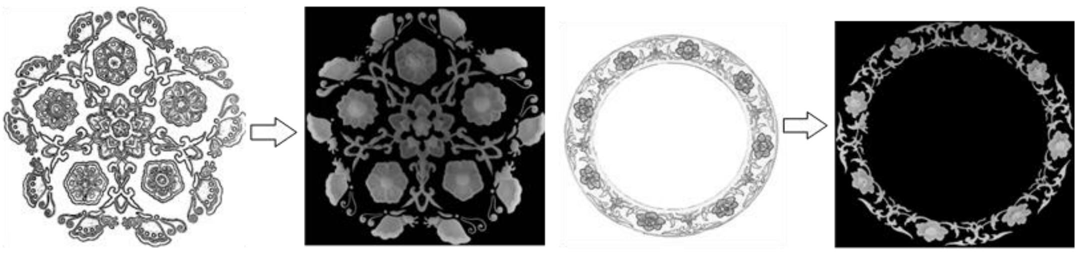

Fig 1 Example of grayscale image generation

3. Quality Assessment and Classification of Grayscale Images

3.1. Multimethod-Based Grayscale Image Quality Parameter Calculation

3.1.1. Statistical method - grayscale variance

Grayscale variance refers to the mean of the squared deviations of all pixel grayscale values from the average grayscale value in an image. This metric reflects the image's sharpness and contrast. A higher grayscale variance indicates greater variation in pixel intensities, suggesting more pronounced grayscale changes within the image and thus higher sharpness and contrast. Conversely, a lower grayscale variance implies smaller fluctuations in grayscale values, indicating lower image clarity and contrast. The calculation formula is as follows:

$$\sigma^2 = \frac{1}{\mathrm{M}\times\mathrm{N}} \times \sum_{\mathrm{x}=0}^{\mathrm{M}-1} \sum_{\mathrm{y}=0}^{\mathrm{N}-1} (I(x,y)-\mu)^2 \tag{1}$$

Where $\mu = \frac{1}{M\times N} \times \sum_{x=0}^{M-1} \sum_{y=0}^{N-1} I(x,y)$ is the average grayscale value of the image, $I(x,y)$ represents the grayscale intensity at pixel location (x,y), M and N denote the number of rows and columns of the image, respectively.

3.1.2. Spatial Domain-Based Method — Tenengrad Gradient

The Tenengrad gradient algorithm is a commonly used method for evaluating image sharpness. Proposed by Tenenbaum, it assesses image clarity based on gradient information. The Tenengrad algorithm assumes that well-focused images have sharper edges and therefore exhibit higher gradient values. It uses the Sobel operator to extract gradient values in both the horizontal and vertical directions, then computes the sum of the squares of these gradients as the evaluation function. A higher Tenengrad value indicates a clearer image. The calculation formula is as follows:

$$Tenengrad = \frac{1}{M\times N} \times \sum_{\mathrm{x}=1}^{M} \sum_{y=1}^{N} G(x,y) \tag{2}$$

Where M and N represent the number of rows and columns of the image, respectively,

$$\mathrm{G(x,y)} = \sqrt{{S_x}^2 + {S_y}^2}, S_x = G_x * \mathrm{I}, S_y = G_y * \mathrm{I}, G_x = \begin{vmatrix} -1 & 0 & 1 \\ -2 & 0 & 2 \\ -1 & 0 & 1 \end{vmatrix}, G_y = \begin{vmatrix} 1 & 2 & 1 \\ 0 & 0 & 0 \\ -1 & -2 & -1 \end{vmatrix}.$$

3.1.3. Entropy Evaluation Function Based on Information Theory

In information theory, entropy is used to describe the richness of information. The entropy evaluation function is based on the grayscale distribution of a focused image. When the grayscale distribution is diverse, pixel grayscale values are widely distributed and show large differences between each other, resulting in high entropy. In contrast, defocused images tend to have lower entropy. Therefore, image clarity can be evaluated using an entropy-based sharpness evaluation function, which is defined as follows:

$$F = \sum_{g=0}^{G} P_k(g) \log_b P_k(g) \tag{3}$$

where b is typically taken as 2, g represents the grayscale value of the image, G denotes the maximum grayscale level, and k refers to the index of a defocused image sequence. $P_k(g)$ is the probability of grayscale level g appearing in the k-th image, calculated as:

$$P_k(g) = \frac{n_g}{M\times N} \tag{4}$$

where M×N represents the total number of pixels in the image, and n_g is the number of pixels with grayscale value g in the k-th image.

3.1.4. Transform Domain Method — Discrete Cosine Transform (DCT)

DCT, as a frequency domain analysis method, transforms the image from the spatial domain to the frequency domain, effectively capturing the frequency characteristics of the image. High-frequency components generally represent image detail information, while low-frequency components reflect the basic structure of the image. Studies have shown that DCT performs well in image quality assessment, effectively capturing the visual features of an image [12]. For an image of size M×N, the sharpness evaluation function based on 2D Discrete Cosine Transform is defined as:

$$E_{dct} = \sum_{u}\sum_{v}(u+v)\,|F(u,v)| \tag{5}$$

where:

$$F(u,v) = a_u a_v \sum_{x=0}^{M-1}\sum_{y=0}^{N-1} f(x,y)cos\frac{(2x+1)u\pi}{2M}cos\frac{(2y+1)v\pi}{2N}$$

$$0\leq u \leq M-1,\ 0\leq v \leq N-1$$

$$a_u = \begin{cases} \frac{1}{\sqrt{M}}, & u=0 \\ \sqrt{\frac{2}{M}}, & 1\leq u\leq M-1 \end{cases},\ a_v = \begin{cases} \frac{1}{\sqrt{N}}, & v=0 \\ \sqrt{\frac{2}{N}}, & 1\leq v\leq M-1 \end{cases}$$

3.2. Grayscale Image Quality Classification and Prediction Based on the K-means Clustering Model

3.2.1. Overview of the K-means Model

In unsupervised learning, the K-Means clustering algorithm is one of the most common methods. Its core idea is to cluster the samples in a dataset into sets of clusters so that the samples within the clusters are closer together and the samples between the clusters are farther apart. The basic process is: first select K clustering centers, calculate the distance between all samples and the center of mass of each cluster, and classify the samples into the closest class; then use the total square error to measure the degree of reasonableness of the clustering, and adjust the center of mass of the clusters if it is not reasonable; and finally, iterate the above process until the convergence of the error so that the distance within the class is as small as possible, and the distance between the classes is as large as possible [13].

3.2.2. Data Preparation

In this study, a K-means clustering model is employed to perform classification and prediction of grayscale image quality. The experimental dataset comprises 131 grayscale images, including 100 high-quality images manually selected (indexed 1–100) and 31 grayscale images generated by artificial intelligence (indexed 101–131). To ensure the objectivity and representativeness of the evaluation, all images were first uniformly converted to a standardized grayscale format. Subsequently, four quantitative grayscale image quality assessment metrics were computed for each image and used as input feature vectors for clustering, thereby establishing a solid foundation for grayscale image quality classification.

3.2.3. Experimental Procedure

By clustering the extracted features with the K-means algorithm, the image can be categorized into two classes: high quality and low quality. The specific steps are as follows:

(1) Feature input: pre-extracted and standardized image quality features are input into the K-Means algorithm, and the number of clusters is set to 2, corresponding to the two categories of high quality and low quality.

ISSN: 1813-4890

(2) Clustering execution: K-Means iteratively calculates the distance between the samples and the clustering center according to the feature space distribution until convergence, and outputs the clustering label of each image.

(3) Result evaluation: the clustered labels are compared with the real quality labels of the images and the classification accuracy is calculated to evaluate the clustering effect.

3.2.4. Experimental Results and Analysis

In the experiment, the initial number of clusters for the K-means algorithm was set to 2. After 100 iterations, the algorithm reached a stable convergence. Among the predictions, 17 images were misclassified in terms of quality, resulting in a final classification accuracy of 87.02%.

Table 1. Clustering results

Category	High quality	Low quality
Picture number	12 3 4 5 6 7 8 9 10 11 12 13 14 15 16 17 18 19 20 21 22 23 24 25 26 27 28 29 30 31 32 33 34 35 36 37 38 39 40 41 42 43 44 45 46 47 48 49 50 51 52 53 54 55 56 57 58 59 60 61 62 63 64 65 66 67 68 69 70 71 72 73 74 75 76 77 78 79 80 81 82 83 84 85 86 87 88 89 90 91 92 93 94 95 96 97 98 99 100 101 102 103 104 105 106 107 108 109 110 111 112 115 116 117 118 119 120 121 122 123 124 125 126 128 129 130 131	113 114 127

In this experiment, as shown in Table 1, the K-Means clustering algorithm successfully classified 114 images into two categories—high quality and low quality—but 17 images were still misclassified, mainly because the quality features of these images are too similar for the algorithm to distinguish them effectively. This indicates that traditional feature-based clustering methods may lack accuracy compared with manual evaluation when image quality differences are subtle.

Among the AI-generated grayscale images, 27 were judged to be of high quality, accounting for 90% of the total. This result indicates that the generated grayscale images show strong stability and reliability in terms of image quality and are able to meet the expected standards in the vast majority of cases. This shows that AIGC has good adaptability and effectiveness in the task of grayscale image generation, which provides a solid foundation for subsequent image analysis and practical sculpting.

4. Validation of the application of grayscale images in ceramic surface engraving modeling

4.1. Experimental design of ceramic surface engraving modeling

In order to systematically assess the feasibility and practicality of AI-generated grayscale images in ceramic engraving modeling, this paper designs a number of experimental stages, including variable control, fine engraving modeling, and toolpath simulation, as illustrated in Fig 2.

1. Variable control: The resolution of all grayscale images is uniformly set to 300 DPI, and the size is standardized to 100 × 100 mm, in order to exclude the interference of size and resolution differences on the modeling quality.

2. Parameter setting of the sculpting software: Based on the industry standard and the recommended value of the software, the height of the surface is set to 2.5 mm in JDSoft Surf Mill 8.0, and the mesh precision is set to 0.04 mm in the X/Y direction.

3. Sample selection: Different sources and grayscale characteristics of the images are selected for comparison experiments, including AI-generated flower and butterfly diagrams and

wreaths, high grayscale level of the dragon and phoenix diagrams, as well as manually drawn portraits, to ensure that the complexity of the pattern is basically the same, so as to facilitate the comparison and analysis.

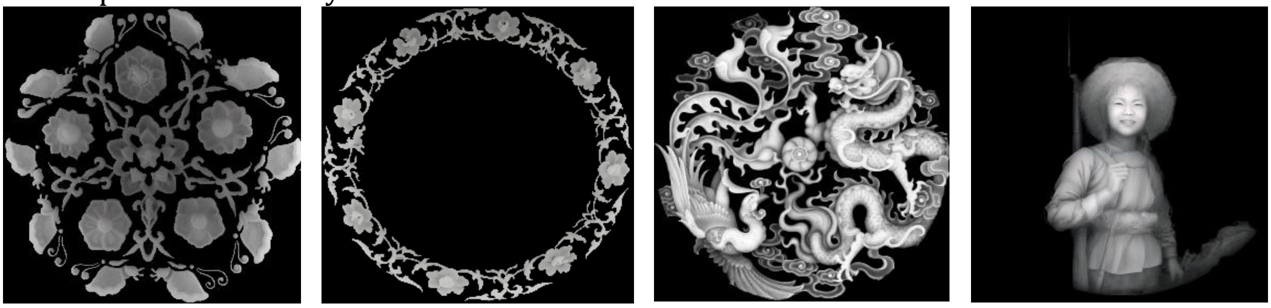

(a) AI-generated flower butterfly (b) AI-generated flower garland (c) High grayscale dragon and phoenix (d) Hand-painted portrait

Fig 2. Sample grayscale drawings

4.2. Experimental Flow

4.2.1. Gray-scale image preprocessing

Import the grayscale image into JDSoft Surf Mill 8.0, scale it to the standard size, and complete the image format conversion to ensure the consistency of subsequent modeling.

4.2.2. Fine engraving modeling and virtual processing

1. Modeling stage: Use the software "Art Surface" function to transform the grayscale image into a three-dimensional relief model.

2. Polishing: Smooth the surface of the model in the virtual sculpture module.

3. tool path simulation: generate the carving tool path, and through the software built-in machine simulation function for the preview of the carving process, while exporting the NC code for subsequent physical verification.

4.3. Experiment and result analysis

4.3.1. AI-generated grayscale image and high-grayscale image of fine engraving modeling experiments - feasibility investigation

In order to explore the feasibility of the combination of AI-generated grayscale image and fine engraving software, this experiment uses the fine engraving software to process the known high grayscale level grayscale images and AI-generated grayscale images under the premise of controlling the experimental variables, and the processed fine engraving images are compared in detail.

The AI-generated grayscale image (flower and butterfly) and the grayscale image with high gray level (dragon and phoenix) under the dot matrix image are imported into the fine engraving software in the 2D drawing workspace, as shown in Fig. (a).

After transforming to a uniform size through scaling, the plane bitmap is converted to a 2D or 3D grid by artistic surface operation, the height of the surface is uniformly set to 2.5mm, and the grid's X (curve) precision and Y (diameter) precision are all set to 0.04mm, and the modeling and rendering display is shown in Fig. (b) of the fine sculpture.

In the virtual sculpture workspace for the overall grinding, so that the effect of sculpture smooth as shown in Fig. (c). Isometric side view is shown in Fig. (d).

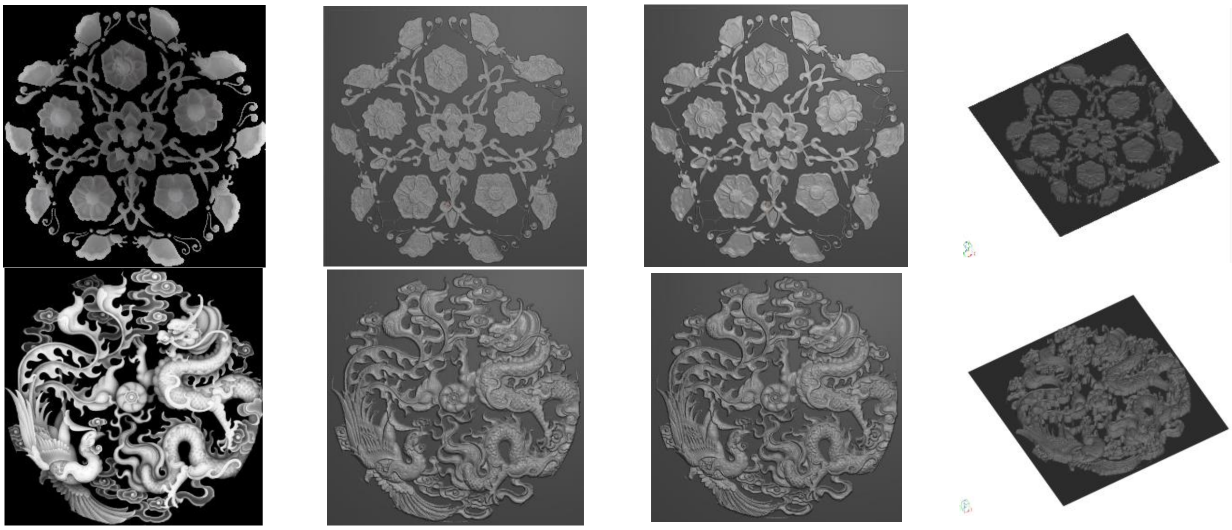

(a) Grayscale drawing (b) Finishing drawing for base modeling (c) Ground finishing drawing (d) Ground finishing isometric view

Fig. 1 Comparison of AI-generated grayscale (flower and butterfly) and high-grayscale (dragon and phoenix) fine engraving effects

Fig. (a) shows that the high grayscale levels of grayscale image layers rich, dark and light demarcation is obvious and clear details, while the AI-generated grayscale image levels are relatively single, dark and light demarcation is not prominent enough, the details of the performance of the fuzzy. Comparison of the two after the fine engraving software base modeling and polishing processing relief image (Fig. (b) and Fig. (c)), high grayscale image of the base modeling relief has been more perfect, polishing processing on the details of the impact is limited; and AI-generated relief image after polishing the details of the more clear, the overall quality of the overall significant improvement, but there is still part of the details are lost. Combined with the isometric side view (Fig. (d)) analysis, high grayscale relief image three-dimensional sense is obvious, while the AI-generated relief image only has a three-dimensional effect of the outer contour, the details of the part is still manifested as a plane. In summary, although the AI-generated grayscale image in the gray level, detail performance and three-dimensional sense is not as good as the existing grayscale image, but after the fine engraving software polishing treatment, the relief surface roughness decreased, proving that AI-generated grayscale image base modeling has a certain degree of feasibility.

4.3.2. Carving tool path machine simulation experiment - usability exploration

After the grayscale image has undergone 2D rendering and virtual sculpting, it can be integrated into a 3D environment. By properly setting the tool paths, the machining simulation performance can be previewed using the built-in machine simulation function of JDSoft Surf Mill 8.0. Alternatively, the NC file can be exported and imported into an NC file viewer to preview and compare the tool path simulation performance, thereby roughly determining whether the grayscale image can be practically applied to machine engraving. The machine simulation performance of the high-gray-level grayscale image (dragon and phoenix) is shown in Fig. 4 (a). while that of the AI-generated grayscale image is shown in Fig. 4 (b). It can be seen that the high-gray-level grayscale image demonstrates better detail performance and stronger stereoscopic effect in the simulation. Although the AI-generated grayscale image is inferior in detail and stereoscopic effect, it still possesses basic engraving features.

ISSN: 1813-4890

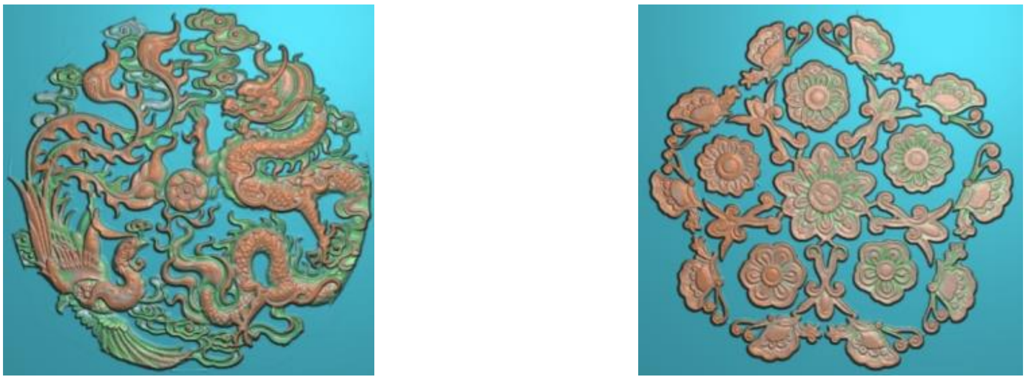

(a) High-gray-level Grayscale Image Machine Simulation - Longfeng

(b) AI-generated grayscale machine simulation - flower and butterfly

Fig.2 Comparison of AI grayscale (flower and butterfly) and high grayscale (dragon and phoenix) engraving knife path machine simulation effect.

The results of this experiment show that with the current experiments using artificial intelligence generated image model, AI-generated grayscale image can be used for carving details and three-dimensional sense of the requirements of the carving is not high carving, and AI grayscale carving height level is simple to make the surface of the relief carving is more flat at the same time to save the carving material, with a certain degree of usability.

4.3.3. Comparison test of manual grayscale image and AI grayscale image - success factor analysis

The manual hand-drawn grayscale image (portrait) and AI-generated grayscale image (wreath) will be processed in the same way as above. The grayscale image, honed and refined image, and honed and refined isometric view are shown in Fig.respectively. Hand-drawn portrait grayscale image grayscale level is obvious, but the boundary is fuzzy, after modeling, the details of a large number of ripples, can not be recovered by simple polishing, need to spend a lot of time to manually trimming processing; AI-generated wreaths grayscale image level is relatively simple, the details of the performance of the general, but only after a simple polishing process, the simulation of the machine tool performance is good.

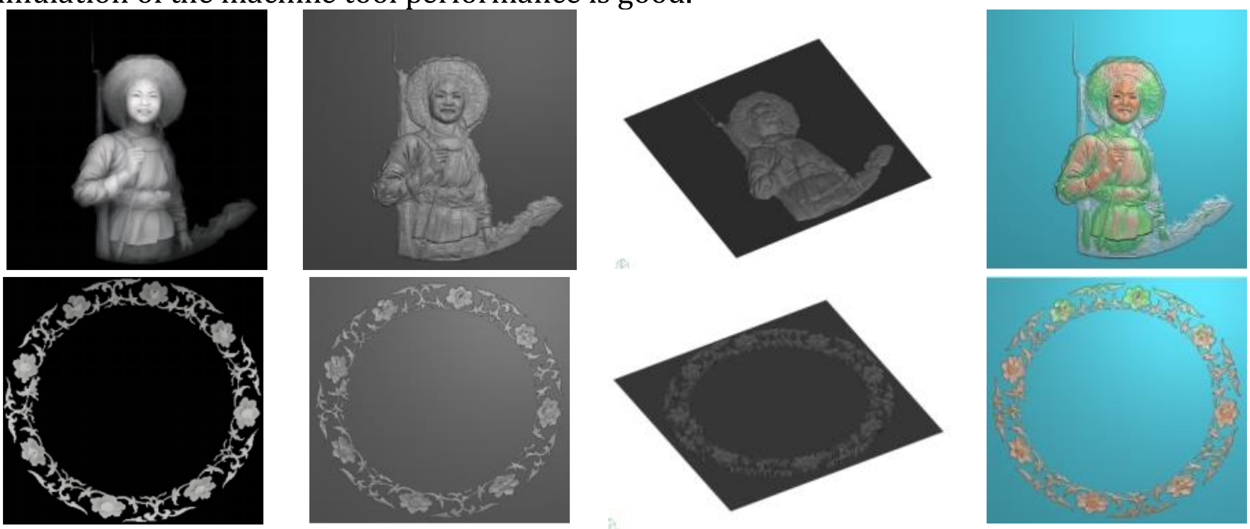

(a)Grayscale image

(b)Polished fine-engraving image

(c)Polished fine-engraving isometric view

(d)Machine-tool simulation image

Fig. 3 Comparison of hand-drawn portrait grayscale image and AI-generated garland grayscale image modeling

Through the above experiments, this chapter can draw a preliminary conclusion that the elements of the success of grayscale image carving are as follows:

ISSN: 1813-4890

1. The grayscale level of the grayscale image cannot be too low: the grayscale level directly affects the richness of the relief level. High grayscale level of grayscale image (dragon and phoenix) can present delicate light and dark transition and three-dimensional details, while the grayscale image generated by the AI model trained in this experiment, the grayscale level is general, the level is more single, resulting in a weak sense of three-dimensionality, and only the outer contour can be presented in three-dimensional effect.
2. Detail clarity and boundary integrity: although the artificial hand-drawn image is rich in levels, but the boundary is fuzzy and easy to cause modeling ripples, requiring complex post-processing; AI generated image details are fuzzy but the boundary is relatively clear, and can be optimized by simple polishing. Clear details and complete boundaries is to reduce tool path anomalies, to ensure the key to engraving accuracy.
3. Noise and distortion control: AI generated image may be due to algorithmic flaws in noise (such as artifacts), which need to be filtered or denoised in pre-processing to improve the quality; an artificial image, if there is a stroke noise, will also lead to modeling errors.
4. Adaptability of engraving software parameters: Surface height (e.g., 2.5mm) and mesh precision (0.04mm) need to be matched with the grayscale resolution (300DPI). Inappropriate parameters will magnify the defects of the grayscale image, such as a low-precision mesh may lose the only details of the AI image.
5. Post-processing feasibility: AI drawings rely on polishing to improve surface smoothness, while the complex ripples of manual drawings need to be manually trimmed. Efficient post-processing capabilities (e.g., virtual sculpting tools) are an important part of making up for the shortcomings of grayscale diagrams.

4.4. Prediction and validation of sculpting results based on success factor analysis

4.4.1. Carving prediction model construction

According to the analysis of the success factors of the experiment and carving mentioned in the previous section, the carving result prediction model is constructed by combining five levels: grayscale level, modeling effect, detail embodiment, boundary clarity, and machine simulation performance.

4.4.2. Actual engraving verification

Combining the above success factors, the AI generated grayscale image (flower and butterfly) is predicted to be "feasible" and the artificial image (portrait) is predicted to be "infeasible" are exported to NC code, and the actual engraving is carried out on the CNC engraving machine.

(a)AI generated grayscale image of a flower and butterfly (b)Relief effect (c)Fired finished product

Fig.4 AI generated grayscale image of the actual engraving of the flower butterfly

The actual carving was found to be the same as the expected results, and the AI generated grayscale image (flower and butterfly) was successfully carved in its entirety, with the finished product shown in Fig.The manual hand-drawn grayscale image (portrait) could not be engraved with a complete finished product, as shown in Fig..

(a)Hand-drawn portrait in grayscale	(b)First time machine carving	(c)Second time machine carving

Fig.5 Hand-drawn portrait grayscale drawing of the actual engravings

5. Conclusion

This paper presents a grayscale image generation and quality evaluation method based on the LoRA (Low-Rank Adaptation) model, which has been successfully applied to ceramic surface engraving modeling. By leveraging LoRA for lightweight fine-tuning of the base image generation model, the proposed approach enables the efficient generation of complex grayscale images suited to ceramic carving tasks, achieving an effective combination of automation and modeling precision. Additionally, a multi-dimensional image quality assessment framework is constructed, integrating information entropy, Discrete Cosine Transform (DCT), grayscale variance, and Tenengrad gradient metrics. This framework, combined with K-means clustering, allows for accurate and interpretable classification of image quality.

Experimental results demonstrate that the proposed method performs well in terms of image quality, computational efficiency, and adaptability, showing strong robustness and generalizability. Although AI generated grayscale images still fall short of hand-drawn images in aspects such as fine detail and depth, they have proven to be highly practical for general engraving needs. Moreover, by analyzing key factors influencing engraving outcomes—such as grayscale level, edge clarity, noise suppression, and software compatibility—this study provides valuable theoretical insights for improving generation models and image quality. Future work will focus on optimizing the LoRA model architecture and expanding the evaluation framework to support more complex applications in industrial image processing and intelligent manufacturing.

Acknowledgements

Upon the completion of my thesis, I would like to extend my sincere thanks to associate professor Tao Liu for his enlightening mentorship and to my project team for their indispensable contributions. I am equally thankful for the financial backing provided by the College Students' Entrepreneurship Training Program 20506004328, which significantly facilitated my research endeavors.

References

[1] J. Ho, A. Jain and P. Abbeel: Denoising Diffusion Probabilistic Models, Advances in Neural Information Processing Systems, Vol. 33 (2020), p.6840–6851.

[2] I.J. Goodfellow, J. Pouget-Abadie, M. Mirza, et al.: Generative Adversarial Nets, Advances in Neural Information Processing Systems, Vol. 27 (2014).

[3] A. Ramesh, M. Pavlov, G. Goh, et al.: Zero-Shot Text-to-Image Generation, Proc. International Conference on Machine Learning (PMLR, 2021), p.8821–8831.

[4] E.J. Hu, Y. Shen, P. Wallis, Z. Allen-Zhu, Y. Li, S. Wang, L. Wang and W. Chen: LoRA: Low-Rank Adaptation of Large Language Models, arXiv:2106.09685 [cs.CL] (2021).

[5] A. Mittal, R. Soundararajan and A.C. Bovik: Making a “Completely Blind” Image Quality Analyzer, IEEE Signal Processing Letters, Vol. 20 (2012) No.3, p.209–212.

[6] Chongqing University: China Patent CN110070539A. (2019).

[7] X.R. Xing: Implementation of Lightweight Image Classification System Based on Binary Discrete Cosine Transform (MS., Xiamen University, China 2020), DOI:10.27424/d.cnki.gxmdu.2020.002284.

[8] B. Wang, Y.P. Sui, H.S. Wang, et al.: Research on Coal Gangue Image Recognition Based on Image Processing and InceptionV3 Neural Network, Shanxi Coking Coal Science & Technology, Vol. 47 (2023) No.3, p.7–11. (In Chinese)

[9] Z. Cao, Y. Chao, W. Xu, et al.: High-Precision Focusing Method for Part Images Based on Improved Gradient Weighting, Journal of Electronic Measurement and Instrumentation, Vol. 37 (2023) No.11, p.132–142. DOI:10.13382/j.jemi.B2306767. (In Chinese)

[10] L. Agnolucci, L. Galteri, M. Bertini, et al.: Arniqa: Learning Distortion Manifold for Image Quality Assessment, Proc. IEEE/CVF Winter Conference on Applications of Computer Vision (2024), p.189–198.

[11] C. Saha and M.F. Hossain: MRI Brain Tumor Images Classification Using K-Means Clustering, NSCT and SVM, Proc. 4th IEEE Uttar Pradesh Section Int. Conf. on Electrical, Computer and Electronics Engineering (UPCON) (Uttar Pradesh, India, 2017), p.329–333.

[12] K.J. Zhou, T. Liao, P. Tan, et al.: A Survey on Image Compression Techniques, Computer Science and Exploration, 1–30 (2025-04-22). Available at: http://kns.cnki.net/ kcms/detail/ 11.5602.TP. 20250310.1405.002.html. (In Chinese)

[13] H.Y. Ma: Research on Hyperspectral Image Classification Algorithm Based on Kmeans-CM (MS., Liaoning Technical University, China 2023), DOI:10.27210/d.cnki.glnju.2023.001029.